# Responses of Contralateral SI and SII in Cat to Same-Site Cutaneous Flutter Versus Vibration

M. TOMMERDAHL,[1] B. L. WHITSEL,[1,2] O. V. FAVOROV,[1] C. B. METZ,[2] AND B. L. O'QUINN[1]
*Departments of [1]Biomedical Engineering and [2]Cell and Molecular Physiology, University of North Carolina, Chapel Hill, North Carolina 27599*

**Tommerdahl, M., B. L. Whitsel, O. V. Favorov, C. B. Metz, and B. L. O'Quinn.** Responses of contralateral SI and SII in cat to same-site cutaneous flutter versus vibration. *J. Neurophysiol.* 82: 1982–1992, 1999. The methods of $^{14}$C-2-deoxyglucose ($^{14}$C-2DG) metabolic mapping and optical intrinsic signal (OIS) imaging were used to evaluate the response evoked in the contralateral primary somatosensory receiving areas (SI and SII) of anesthetized cats by either 25 Hz ("flutter") or 200 Hz ("vibration") sinusoidal vertical skin displacement stimulation of the central pad on the distal forepaw. Unilateral 25-Hz stimulation consistently evoked a localized region of elevated $^{14}$C-2DG uptake in both SI and SII in the contralateral hemisphere. In contrast, 200-Hz stimulation did not evoke elevated $^{14}$C-2DG uptake in the contralateral SI but evoked a prominent, localized region of increased $^{14}$C-2DG uptake in the contralateral SII. Experiments in which the OIS was recorded yielded results that complemented and extended the findings obtained with the 2DG method. First, 25-Hz central-pad stimulation evoked an increase in absorbance in a region in the contralateral SI and SII that corresponded closely to the region in which a similar stimulus evoked increased $^{14}$C-2DG uptake. Second, 200-Hz stimulation of the central pad consistently evoked a substantial increase in absorbance in the contralateral SII but very little or no increase in absorbance in the contralateral SI. And third, 200-Hz central-pad stimulation usually evoked a decrease in absorbance in the same contralateral SI region that underwent an increase in absorbance during same-site 25-Hz stimulation. Experiments in which the OIS responses of both SI and SII were recorded simultaneously demonstrated that continuous (>1 s) 25-Hz central-pad stimulation evokes a prominent increase in absorbance in *both* SI and SII in the contralateral hemisphere, whereas *only* SII undergoes a sustained prominent increase in absorbance in response to 200-Hz stimulation to the same central-pad site. SI exhibits an initial, transient increase in absorbance in response to 200-Hz stimulation and at durations of stimulation >1 s, undergoes a decrease in absorbance. It was found that the stimulus-evoked absorbance changes in the contralateral SI and SII are correlated significantly during vibrotactile stimulation of the central pad—positively with 25-Hz stimulation and negatively with 200-Hz stimulation. The findings are interpreted to indicate that 25-Hz central-pad stimulation of the central pad evokes spatially localized and vigorous neuronal activation within both SI and SII in the contralateral hemisphere and that although 200-Hz stimulation evokes vigorous and well maintained neuronal activation within the contralateral SII, the principal effect on the contralateral SI of a 200-Hz stimulus lasting >1 s is inhibitory.

## INTRODUCTION

There is general agreement that in cats and monkeys (and presumably in humans) the spike discharge activity a mechanical stimulus sets up in rapidly adapting (RA), slowly adapting (SA), and Pacinian (PC) skin mechanoreceptors is projected centrally, at short latency and with relatively minor transformation, to primary somatosensory cortex (both SI and SII) in the contralateral hemisphere. There is no consensus, however, about the way in which the stimulus-evoked response in each area contributes to cerebral cortical somatosensory information processing and somatosensation.

According to current models, the principal source of the input that enables SII to respond to contralateral mechanoreceptor afferent drive is different in different species. In cats, for example, most input to SII from the opposite side of the body is conveyed via thalamocortical connections (the "in-parallel" model) (Rowe et al. 1996). In old world primates, however, the main input to SII from the opposite side of the body is conveyed via corticocortical axons arising in SI of the same hemisphere (the "serial" model) (Burton 1995; Pons et al. 1987). While the "in-parallel" or "serial" models of somatosensory information flow account for the sources of input to SI and SII, neither model addresses the important issue of whether, and to what extent, the activity evoked in one cortical area by a skin stimulus is independent of the activity the same stimulus evokes in the other.

The experiments described in this paper are a component of the initial stage of a program of research designed to obtain detailed information bearing directly on this issue. To this end, the 2-deoxyglucose (2DG) and optical intrinsic signal (OIS) imaging methods were employed to evaluate the locus, form, magnitude, and time course of the responses of SI and SII in the contralateral hemisphere of cats to 25 versus 200-Hz vertical displacement stimulation of the central pad. A recent related study (Tommerdahl et al. 1999) described the responses of contralateral anterior parietal cortex in squirrel monkey to 25- and 200-Hz stimulation of the same skin site.

## METHODS

### *Subjects and preparation*

Subjects were adult cats (males and females). All surgical procedures were carried out under general anesthesia (1–4% halothane in a 50/50 mixture of oxygen and nitrous oxide). After induction of anesthesia, the trachea was intubated with a soft tube, and a polyethylene cannula was inserted in the femoral vein to allow administration of drugs and fluids (5% dextrose and 0.9% NaCl). No further surgical manipulations were required in the subjects in which 2DG imaging was carried out. For each subject used for OIS imaging, a 1.5-cm-diam opening was made in the skull overlying somatosensory cortex, a chamber was mounted to the skull over the opening with dental acrylic, and the dura overlying anterior parietal cortex was incised and removed. All wound margins were infiltrated with long-lasting local anesthetic, the skin and muscle incisions were closed with sutures, and

The costs of publication of this article were defrayed in part by the payment of page charges. The article must therefore be hereby marked "*advertisement*" in accordance with 18 U.S.C. Section 1734 solely to indicate this fact.

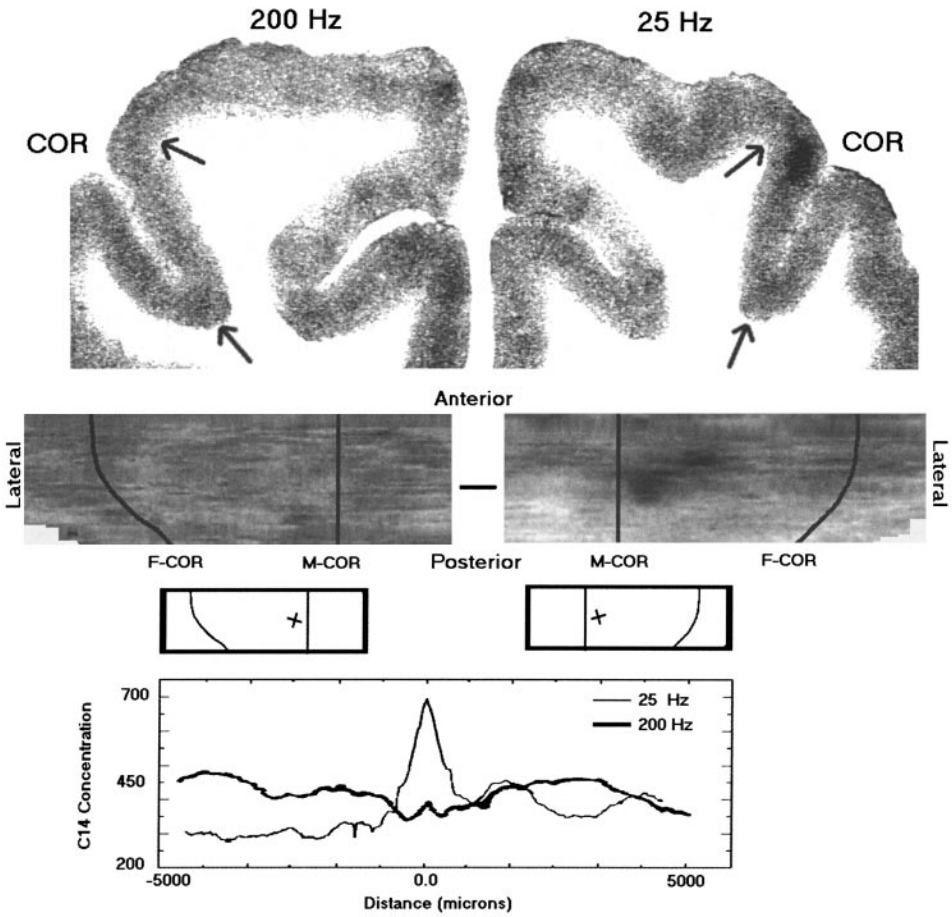


FIG. 1. *Top*: digitized image of autoradiograph of section that includes portions of both the right and left hemispheres. *Right side* of the image shows distribution of $^{14}$C-2-deoxyglucose ($^{14}$C-2DG) in the hemisphere contralateral to the 25-Hz central-pad stimulus; *left side* of the image shows the distribution of label in the hemisphere contralateral to the 200-Hz central-pad stimulus. Top arrow on each side of image, locus of point of maximal curvature of cortex in medial bank of coronal sulcus (M-COR); bottom arrow on each side of image, locus of fundus of coronal sulcus (F-COR). *Middle*: unfolded maps showing the distribution of $^{14}$C-2DG in left (on the *left*) and right (on the *right*) pericoronal cortex in the same subject. Note the presence of elevated 2DG uptake (black region) in the map for pericoronal cortex contralateral to the 25-Hz stimulus and the absence of regions of elevated 2DG uptake in the map of pericoronal cortex contralateral to the 200-Hz stimulus. *Insets*: × depicts locus of the reference point used to generate the [$^{14}$C] vs. distance plots shown at *bottom*. *Bottom*: variation in $^{14}$CDG concentration as a function of distance from reference point 0.0. Note that 200-Hz stimulation was associated with below-background $^{14}$C-2DG concentration values in the same SI region maximally activated by same-site 25-Hz cutaneous flutter.

each surgical site outside the recording chamber was covered with a bandage held in place by adhesive tape.

Before (1–3 h prior to) the data acquisition phase of the OIS-imaging experiments or to administration of $^{14}$C-2DG, subjects were immobilized with Norcuron (vecuronium bromide; loading dose 0.1–0.5 mg/kg; 0.5 $\mu g \cdot kg^{-1} \cdot min^{-1}$ thereafter). At all times thereafter subjects were ventilated using a 50/50 oxygen and nitrous oxide mix; supplemented with 0.1–1.0% halothane. Respirator rate and volume were adjusted to maintain end-tidal $CO_2$ between 3.0 and 4.0%; electroencephalographic and autonomic signs (slow wave content; heart rate, etc.) were monitored and titrated (by adjustments in the anesthetic gas mix) to maintain levels consistent with light general anesthesia. Rectal temperature was maintained (using a heating pad) at 37.5°C.

The cats were killed by intravenous injection of pentobarbital (45 mg/kg) and by intracardial perfusion with saline followed by fixative (10% formalin). After perfusion, fiducial marks were placed to guide removal, blocking, and subsequent histological sectioning of the cortical region studied. All procedures were reviewed and approved in advance by an institutional committee and are in full compliance with current National Institutes of Health policy on animal welfare.

### *Stimuli and stimulus protocols*

In all but one of the 2DG and OIS-imaging experiments that provided the data reported in this paper, the mechanical stimuli used to evoke cortical activity were applied to the same site (a 5-mm-diam site in the center of the central pad of the distal forepaw) on the forelimb. In the one subject in which a skin site different from the central pad was stimulated (an experiment using the OIS-imaging method), the stimuli were applied to a 5-mm site on the hairy skin of the ventral ulnar forelimb at the level of the pisiform pad. The stimuli always consisted of sinusoidal vertical skin displacements applied using a servocontrolled transducer (Cantek Metatron, Canonsburg, PA).

Two frequencies of sinusoidal vertical displacement stimulation were used in most experiments—25 and 200 Hz. In the initial 2DG experiments (3 subjects), one of the frequencies was delivered to one forepaw central pad and the other frequency to the corresponding site on the central pad of the opposite forepaw. In the second series of 2DG experiments (2 subjects), 200-Hz stimulation was applied unilaterally to the central forepaw. In all but one OIS-imaging experiments, the stimuli (25 and 200 Hz) were delivered to the same skin site (the central pad) used in the 2DG studies, and in every experiment the different frequencies of stimulation were interleaved in the same "run" on a trial-by-trial basis. To illustrate, in the initial trial of such a run, the 25-Hz stimulus (10-s duration) was followed by a 50-s interstimulus interval (ISI); in the second trial, the 200-Hz stimulus (10 s in duration) was followed by a 50-s ISI, etc. Twenty to 100 trials were delivered in each run.

Parameters of the 25-Hz stimulus used in the OIS-imaging experiments were as follows: peak-to-peak amplitude, 400 $\mu$m; duration, 3–15 s; intertrial interval (ITI), 60 s. The parameters of the 200-Hz stimulus were: peak-to-peak amplitude, 40 $\mu$m; duration, 3–15 s; ITI, 60 s. The stimuli were applied by means of a 5-mm-diam, cylindrical Delrin probe, which in every experiment made continuous contact with the skin. In the periods during which no sinusoidal skin displacements were delivered (the intertrial and interrun intervals, respectively), the stimulator probe indented the pad by 500 $\mu$m.

### *2DG imaging*

In the 2DG experiments, mechanical skin stimulation was applied continuously for 0.5–1 h before and for 45 min after pulse intravenous injection of the tracer (300–500 $\mu$Ci/kg of $^{14}$C-2DG). The period of

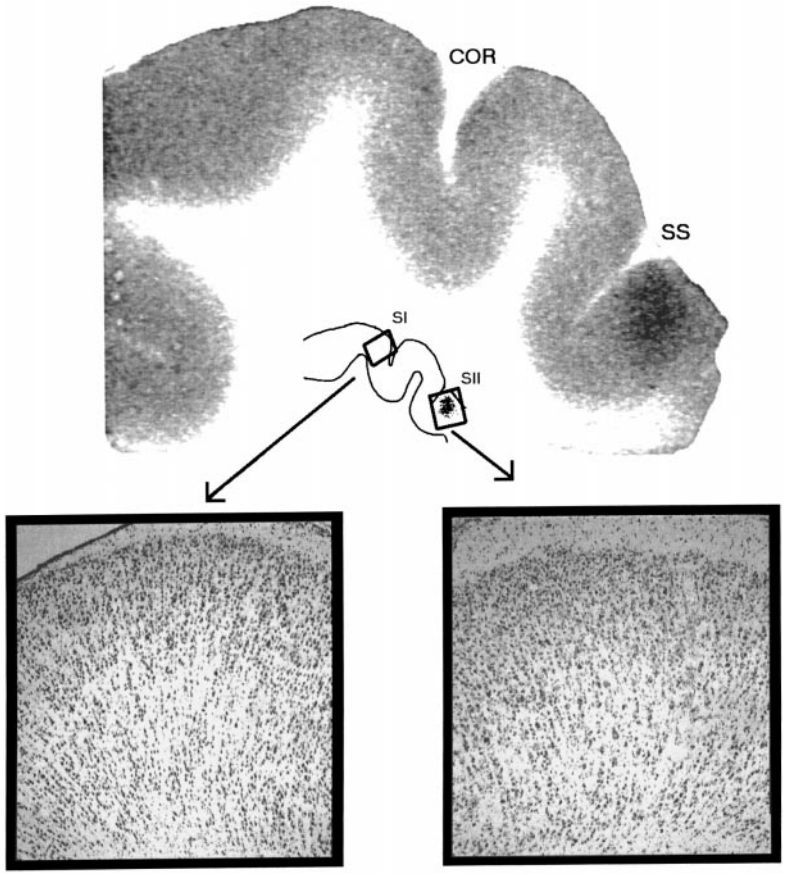


FIG. 2. *Top*: image of an autoradiograph generated from section cut from the right hemisphere of a cat that received 200-Hz stimulation on the central pad of the left forepaw. Section includes both SI and SII. Region of above-background $^{14}$C-2DG labeling at right edge of image is evident; this region is within SII. *Bottom*: images of Nissl-staining illustrating cytoarchitecture in the SI (*left*) and SII (*right*) regions in the section from which the image shown at the *top* was obtained. Boxes on outline drawing of section shows regions from which the images of cytoarchitecture were obtained.

2DG labeling was terminated by pentobarbital administration (40 mg/kg iv) followed by intracardial perfusion with saline and fixative. A tissue block including SI and SII in both hemispheres was removed, frozen by immersion in liquid Freon cooled to −50°C, and stored in a low-temperature freezer (−70°C). Coronal sections were cut in the coronal plane at 30 $\mu$m, placed on coverslips, dehydrated, glued to cardboard, and exposed to X-ray film (Juliano et al. 1981, 1983; Tommerdahl et al. 1993, 1996).

Autoradiographs of the distribution of $^{14}$C labeling in cortical sections were viewed with a macroscope fitted with a CCD camera (Fairchild CCD3000; 488 × 380 element sensor). The camera generated a standard RS-170 video signal that was digitized using an imaging board (Datacube; resolution of 768 × 512 × 8 bits at 30 frames/s). A digital computer and custom-designed image analysis software allowed conversion of film optical density values to $^{14}$C concentrations and calibration, collection, display, storage, and analysis of imaging data (Tommerdahl 1989; Tommerdahl et al. 1985, 1993, 1996).

For each autoradiograph, an average $^{14}$C concentration value was determined for each of a continuous series of radially oriented, rectangular bins (bin height 1,000 $\mu$m; binwidth 100 $\mu$m) spanning the full mediolateral extent of pericoronal cortex. This procedure ("image segmentation") (Tommerdahl 1989; Tommerdahl et al. 1985, 1993, 1996) yields a series of $^{14}$C values, one for each radial bin (segment). Each radial bin was centered on layer IV to ensure that each average [$^{14}$C] value used to form a map of the tangential distribution of label in pericoronal cortex is based on a data sample that relates to the locus of maximal input drive in the same way as the samples derived from all other bins.

An unfolded map of the tangential distribution of $^{14}$C-2DG in pericoronal cortex of each subject was reconstructed. Such a map always included the entire region of pericoronal cortex expected to receive input from the stimulated skin site and was generated from the data sampled at relatively low resolution (20–40 pixels/mm) from 50–100 autoradiographic images. The data array (the series of average [$^{14}$C] values generated by segmenting pericoronal cortex in an autoradiographic image) was aligned with the arrays obtained from neighboring images by using a morphological boundary identifiable in all images—the point of maximal curvature of the medial wall of the coronal sulcus (M-COR). Alignment of the data arrays in this way is a requirement for generation (using custom-designed graphics software) (Tommerdahl 1989; Tommerdahl et al. 1985) of a two-dimensional "unfolded" map of the tangential distribution of 2DG labeling within the cortical region of interest (e.g., Fig. 1). Within such an unfolded map a single horizontal pixel string corresponds to the mediolateral array of average [$^{14}$C] values sampled from a single image.

### *OIS imaging*

Near-infrared (IR; 833 nm) OIS imaging was carried out using an oil-filled chamber capped with an optical window (Tommerdahl and Whitsel 1996; Tommerdahl et al. 1998, 1999). Images of the exposed cortical surface were acquired 200 ms before stimulus onset ("reference" or "prestimulus" images) and continuously thereafter ("poststimulus" images; at a resolution of 1 image every 0.9–1.4 s) for 15–20 s after stimulus onset. Exposure time was 200 ms.

OIS difference images were generated by subtracting the prestimulus image from its corresponding poststimulus image. Averaged difference images typically show regions of both increased absorption of IR light and decreased absorption of light that have been shown (e.g., Grinvald 1985; Grinvald et al. 1991; 1994; for review, see Ebner and Chen 1995; also Tommerdahl et al. 1998, 1999) to be accompanied by increases and decreases in neuronal activation, respectively. Difference images of the SI response to stimulation of the same skin site with 25- and 200-Hz stimulation were generated only from data obtained in the same experimental run using the interleaved trial approach described above—this restriction served to control for temporal changes in cortical "state" unrelated to stimulus conditions that,

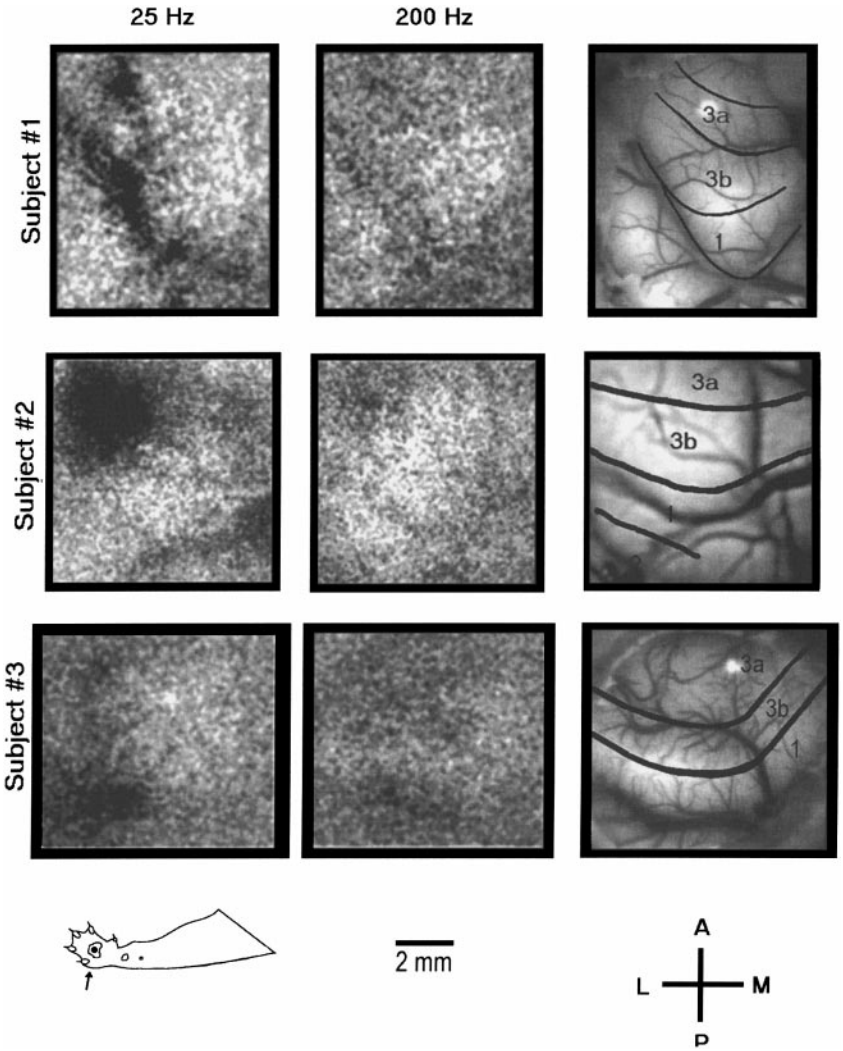


FIG. 3. *Left* and *middle*: average prestimulus-poststimulus difference images obtained from the contralateral SI in 3 subjects. All images were obtained at 5 s after stimulus onset. *Left*: images were generated from the data obtained in 20–40 trials in which a 25-Hz sinusoidal (400 $\mu$m peak to peak) stimulus was delivered. *Middle*: images were generated from the data obtained in 20–40 trials using a 200-Hz (40 $\mu$m peak to peak) stimulus to the same site. Intertrial interval (ITI) was 60 s. *Right*: locations of cytoarchitectonic boundaries (black lines) superimposed on image of surface vascular pattern. For all 3 subjects, each frequency of stimulation was applied to the same site on the central pad. Although 25-Hz stimulation evoked a prominent increase in absorbance in the topographically appropriate region of SI (indicated by dark regions in the images), 200-Hz stimulation did not.

if unrecognized, might obscure or modify the optical response evoked by one or both stimulus frequencies.

The relationship between the optical responses of SI and SII in the contralateral hemisphere was evaluated by correlation mapping (Tommerdahl et al. 1998). A correlation map was formed by choosing a reference region within the OIS image and computing the intensity correlation $r_{ij}$ between the absorbance value of each pixel ($i$, $j$) and the average absorbance within the reference region over time after stimulus onset. The region in the image selected as the reference was the region in SI or SII defined by the boxel (typically, 2 × 2 mm) for which average absorbance underwent the largest increase during skin stimulation. Each pixel ($i$, $j$) in a correlation map is represented by a correlation value $r_{ij}$ ($-1 < r < +1$). In other words, each pixel in such a correlation map shows the value of the correlation between the time course of the OIS in the reference boxel and the time course of the OIS measured at that pixel location. The statistical significance of the computed correlations was evaluated using the standard $t$-test.

### *Histological procedures/identification of cytoarchitectural boundaries/reconstruction of the relationships between cytoarchitecture and the 2DG and OIS-imaging observations*

2DG IMAGING. Coronal sections (30-$\mu$m thickness) were cut from the block of cerebral cortex obtained from each subject studied using the 2DG method; each block included SI and SII in both hemispheres. After production of an autoradiographic image (on X-ray film) of the distribution of $^{14}$C-2DG within each section, each section was removed from the coverglass used to maintain it in stable contact with the X-ray film and was Nissl-stained with cresyl fast violet (for details, see Tommerdahl et al. 1993, 1996; also Juliano et al. 1981, 1983). The stained sections were remounted on slides (serial order was preserved), coverslipped, and examined microscopically to determine the locations of cytoarchitectonic boundaries. Cortical cytoarchitecture in the vicinity of the SI or SII region in which the stimulus evoked above-background 2DG uptake was identified using established criteria (for SI, Hassler and Muhs-Clement 1964; Juliano et al. 1981; McKenna et al. 1981; for SII, Burton et al. 1982; Juliano et al. 1983). The relationship between 2DG uptake and cortical cytoarchitectonic boundaries in each brain was reconstructed using approaches described in detail in previous publications (Juliano et al. 1981, 1982; Tommerdahl et al. 1993, 1996).

OIS IMAGING. In each experiment, a block of tissue that included the region(s) in the contralateral hemisphere from which OIS responses had been obtained was removed after intracardial perfusion with saline and fixative. The block then was postfixed, cryoprotected, and frozen, and serial sections were cut in the coronal plane (30-$\mu$m thickness). The sections were Nissl-stained with cresyl fast violet. The locations of cytoarchitectural boundaries in sections at a series of levels within the territory from which imaging data had been obtained were identified using the criteria described in the preceding paragraph. For each subject, the relationship between the OIS-imaging results and cortical cytoarchitecture was reconstructed using approaches described in detail in previous papers (Tommerdahl et al. 1998, 1999).

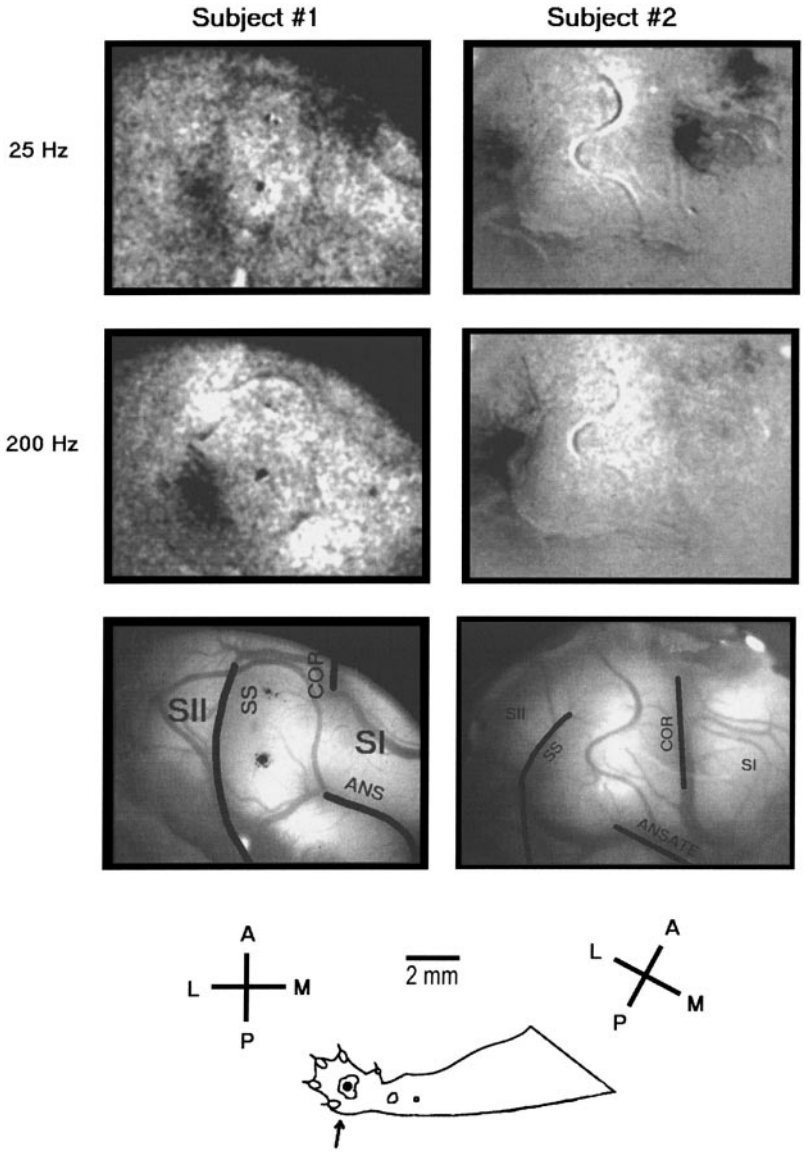


FIG. 4. OIS-imaging results obtained from 2 subjects. *Top*: difference images from 2 subjects showing the responses of both SI and SII in the hemisphere contralateral to 25-Hz central-pad stimulation. Note that responding region of SI is located at *top right* of each image; and responding region of SII is located at *bottom left*. *Middle*: difference images from the same 2 subjects showing the responses of SI and SII in the hemisphere contralateral to 200-Hz central-pad stimulation. *Bottom*: each panel shows the superimposed thresholded responses of a subject to 25-Hz (black code) and to 200-Hz (gray code) stimulation (threshold was set to reveal only those absorbance values equal to or exceeding 5% of maximum). Diagram *below* panels shows surface vascular patterns with locations of sulci enhanced by bold lines. COR, coronal sulcus; SS, suprasylvian sulcus; ANS, ansate sulcus. Scale, orientation of images, and locus of skin stimulus indicated at *bottom*.

## RESULTS

### *2DG-imaging experiments*

The digitized image of the autoradiograph at the *top* of Fig. 1 reveals the distribution of $^{14}$C-2DG uptake within a single coronal section. The section used to produce this autoradiograph was obtained at an anteroposterior level that included the region of SI in both the right and left hemispheres that receives its input from the skin of the distal forelimb. The stimulus condition used to evoke the localized $^{14}$C-2DG uptake apparent in this image (dark regions indicate regions of high $^{14}$C-2DG uptake) was uninterrupted 25-Hz stimulation of the central pad on the left forepaw and, simultaneously, continuous 200-Hz stimulation of the central pad on the right forepaw.

A distribution of $^{14}$C-2DG uptake in SI similar to that in the image at the *top* of Fig. 1 was obtained in all three subjects studied in the same way. Specifically, a prominent column-shaped patch of elevated uptake extending continuously between layers II and V was present in the superficial part of the medial bank of the coronal sulcus (M-COR) in the right hemisphere—the location of this patch of tracer accumulation in the right hemisphere of the image shown in Fig. 1 (and in the hemisphere contralateral to the 25-Hz stimulus in the other 2 subjects—not shown) occupies a territory in SI demonstrated by previous receptive-field mapping studies to receive its principal afferent input from the skin of the contralateral central pad (e.g., McKenna et al. 1981). In contrast, no region(s) within the topographically corresponding region of SI in the hemisphere contralateral to the central pad that received 200-Hz stimulation (e.g., left hemisphere in the image at *top* of Fig. 1) exhibited above-background $^{14}$C-2DG uptake in any of the three subjects.

Immediately below the digitized image at the *top* of Fig. 1 are two unfolded maps, each showing the tangential distribution of labeling (in terms of [$^{14}$C] values; depicted in grayscale) within the pericoronal cortex of one hemisphere. Both of the unfolded maps in Fig. 1 were generated from the data (average [$^{14}$C] values at each of a series of locations in each of a large number of images; 110 images were used for the map on the *right*, 85 for the map on the *left*) obtained from coronal sections separated by no more than 150 $\mu$m.

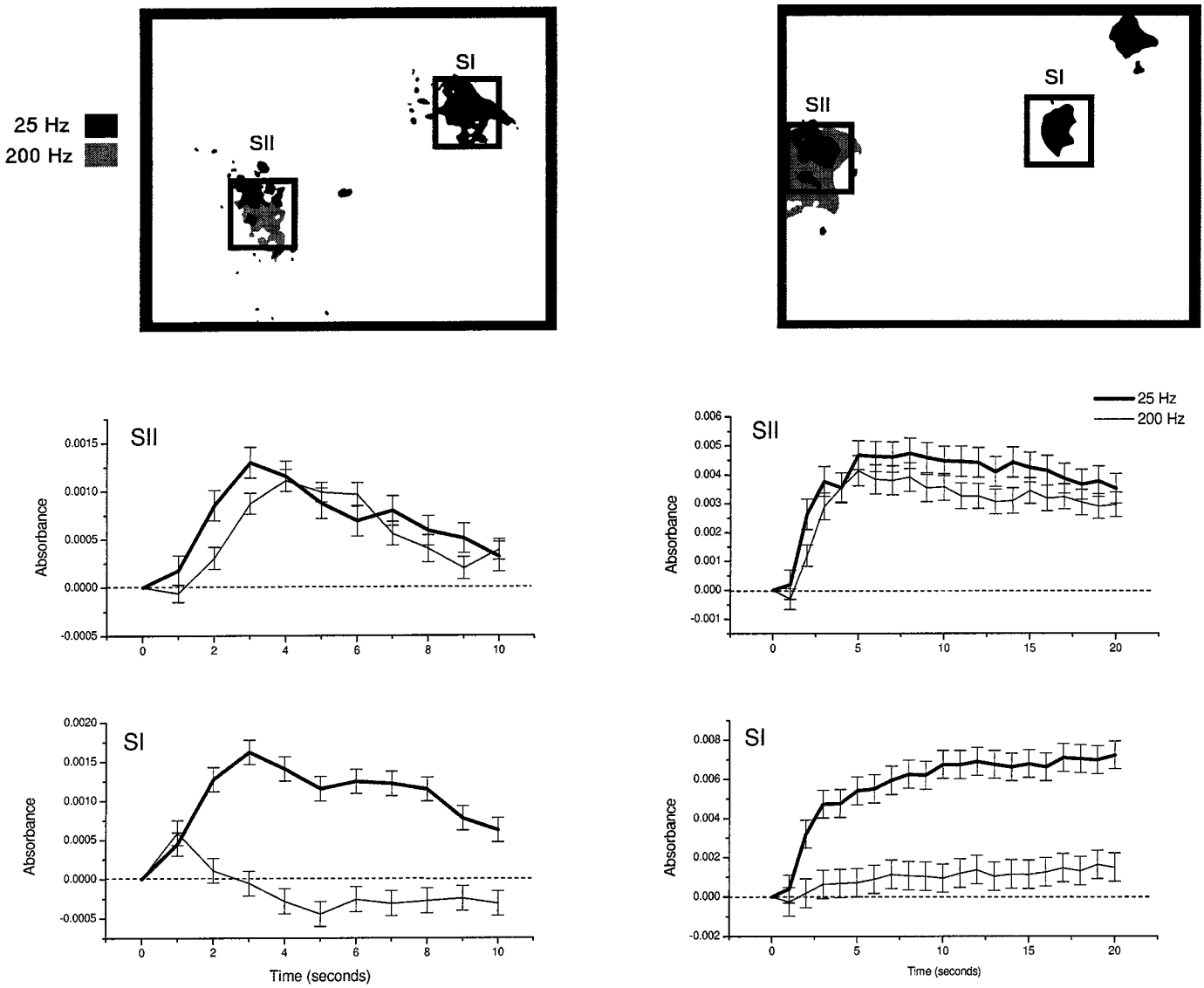


FIG. 5. SI and SII in the contralateral hemisphere respond similarly to 25-Hz stimulation but differentially to 200-Hz stimulation. Time course of the optical responses to 25- and 200-Hz stimulation at selected sites (boxels) in SI and SII of same subjects whose data are shown in Fig. 4. *Subject 1*'s data shown at *left; subject 2*'s data shown on *right. Top*: location of the SI and SII regions in each subject in which absorbance increased during 25-Hz (black code) and 200-Hz (gray code) skin stimulation. Locations of the 2 × 2mm boxels within which a measurement of average absorbance was obtained at multiple time points after onset of skin stimulation indicated by rectangles. *Top graphs*: time course of absorbance changes measured within the 2 × 2mm boxel in SII of each subject to 25-Hz stimulation (heavy lines) and to 200-Hz stimulation (thin lines). *Bottom graphs*: time course of absorbance changes measured within the SI boxel of each subject during same-site 25-Hz stimulation (heavy lines) and 200-Hz stimulation (thin lines).

Inspection of the unfolded 2DG maps in Fig. 1 confirms, for the same subject that provided the image of the single section shown at the *top* of the same figure, that the distribution of $^{14}$C-2DG uptake in the hemisphere contralateral to the 25-Hz stimulus (map at *right* of Fig. 1) includes a prominent region of above-background tracer accumulation where SI cortex folds to form the medial bank of the coronal sulcus (M-COR), and that an absence of above-background uptake at *all* SI locations contralateral to the skin site that received 200-Hz stimulation (map at *left* of Fig. 1). In addition, the two plots in Fig. 1, *bottom*, allow direct comparison of the tangential distribution of $^{14}$C-2DG uptake in SI in the two hemispheres—more specifically, these two plots show how average $^{14}$C-2DG uptake (average [$^{14}$C]) varies as a function of increasing radial distance (binwidth = 7 $\mu$m) from a reference point common to both maps. The reference point for the $^{14}$C concentration values plotted with the thin line is the mediolateral position at which $^{14}$C-2DG uptake is maximal in the map of SI contralateral to the 25-Hz central-pad stimulus—this position is designated as 0.0 on the *x* axis and is identified by the × located in the *inset* below the unfolded map on the *right*. Similarly, the mediolateral location of the topographically corresponding point in the unfolded map of SI contralateral to the 200-Hz stimulus (identified by superimposing the unfolded maps for left and right pericoronal cortex) is also at the 0.0 point on the *x* axis, and average $^{14}$C concentration value in this unfolded map is plotted (heavy line) as a function of increasing radial distance from the reference point (point × in the *inset* diagram

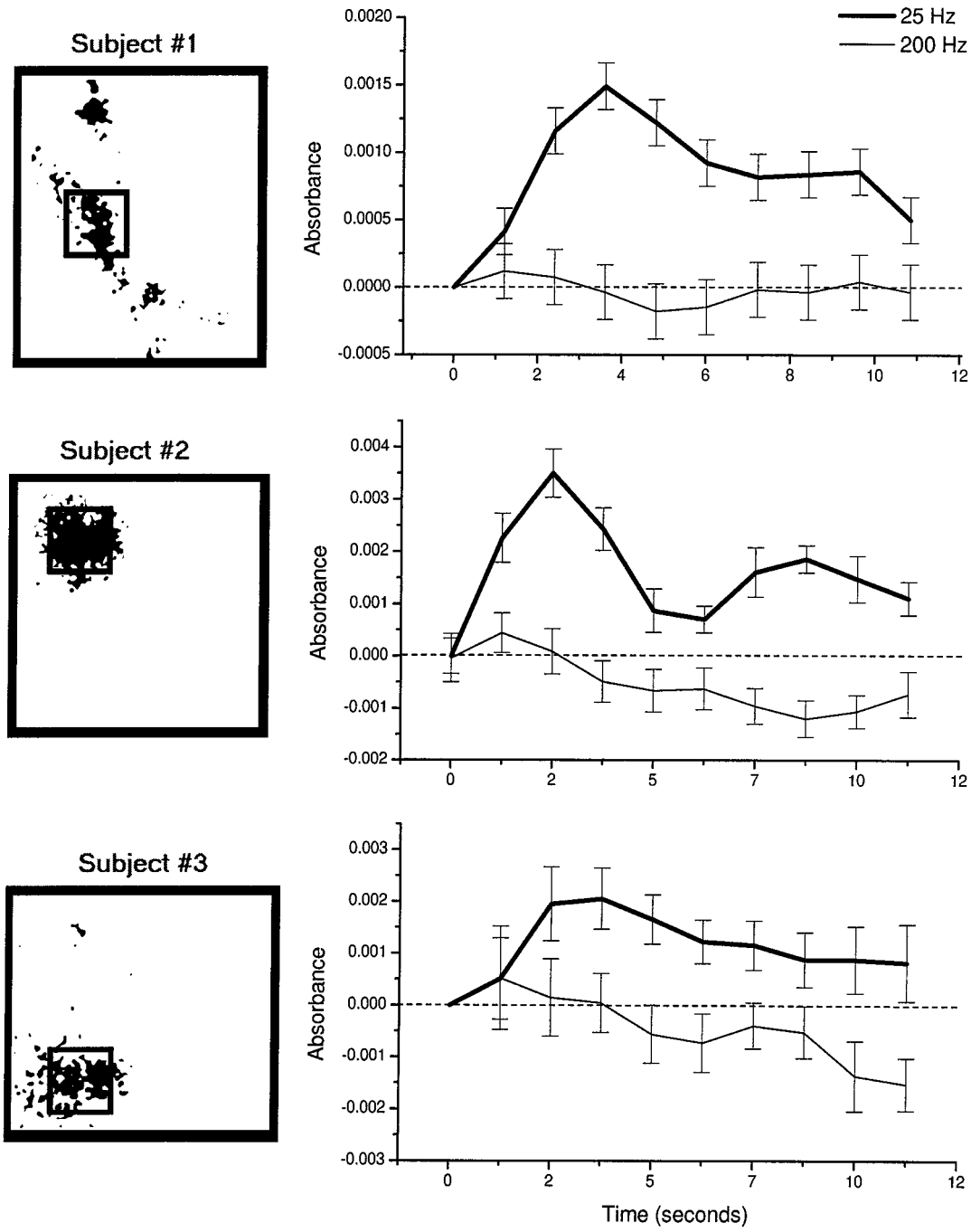


FIG. 6. Differential OIS response of the contralateral SI to 25- and 200-Hz stimulation in 3 different subjects. Data from 3 subjects are shown. Each pair of graphs at *right* was obtained from the data of a single subject. *Left*: thresholded response (black code; image obtained at 5 s after stimulus onset) of SI of each subject to 25-Hz stimulation—the location of the boxel within which average absorbance was determined at different times after stimulus onset is indicated by the rectangle. Graphs show the time course of the changes in absorbance in the 2 × 2 mm SI boxel within which the maximal average absorbance increase occurred during 25-Hz stimulation (heavy lines); thin lines show the time course of the change in absorbance measured within the same boxel during 200-Hz stimulation.

of the unfolded map shown on the *left* immediately *above* the *bottom panel* in Fig. 1).

Briefly summarized, the [$^{14}$C] versus distance plots in Fig. 1, *bottom*, show that the spatial distribution of $^{14}$C-2DG uptake in SI of the hemisphere contralateral to the 25-Hz stimulus (thin line) included a prominent and spatially localized region of elevated uptake (~1.7 mm in diameter, located near to the top of the medial bank of the coronal sulcus). In contrast, at all locations in SI of the hemisphere contralateral to the 200-Hz stimulus (plot with heavy line Fig. 1, *bottom*) uptake did not differ substantially from background. Background $^{14}$C-2DG uptake was estimated as the average [$^{14}$C ] observed at locations >3 mm in all directions from the point of maximal uptake (point 0,0)—for the data shown in Fig. 1, this approach to

estimating background yields essentially the same result for both hemispheres.

A somewhat different design was used in two additional subjects studied using the 2DG mapping method. Specifically, in these experiments a 200-Hz stimulus was delivered to the central pad on the right forelimb; no stimulus was delivered to the left forelimb; and a plane of cortical section was used that included the central-pad representational territory in both SI *and* in SII of the hemisphere contralateral to the skin site that received 200-Hz stimulation. It was anticipated that this design would provide data bearing on a possibility that cannot be rejected on the basis of the data shown in Fig. 1—the lack of a region of elevated $^{14}$C-2DG uptake in SI in the hemisphere contralateral to 200-Hz stimulation might have been due to a failure to deliver an effective 200-Hz skin stimulus.

Figure 2 shows a representative image (at the *top*) showing the distribution of $^{14}$C-2DG in a section from one of the two subjects studied using the design described in the preceding paragraph. Note the prominent column-shaped profile of above-background uptake in the contralateral SII and the absence of above-background label in SI in the same hemisphere. The importance of this outcome is that it not only demonstrates that the 200-Hz stimulus evoked significant afferent drive that activated SII in the contralateral hemisphere, but it reveals that the same 200-Hz stimulus did *not* cause significant activation of the contralateral SI. In all subjects studied with the 2DG method ($n = 5$; 3 using the design illustrated in Fig. 1, 2 using the design shown in Fig. 2), 200-Hz stimulation of the central pad evoked above-background labeling in SII in the hemisphere contralateral to the stimulated skin site but failed to evoked appreciable uptake in the contralateral SI.

### *OIS-imaging experiments*

Figure 3 shows OIS imaging results obtained from three subjects—the images obtained from the same subject occupy a single row. In all three subjects, the 25-Hz contralateral central-pad stimulus (Fig. 3, *left*) evoked a prominent increase in absorbance that was most prominent in areas 3b and 1 but also involved area 3a. The fact that the region exhibiting an increase in absorbance evoked by 25-Hz stimulation appears to be more spatially extensive in one subject (*subject 2*) than the region in which absorbance was increased in the other two subjects is interpreted as attributable mainly to the fact that in *subject 2* the entire responding area occupies exposed cortex, whereas in both of the other subjects, a significant portion of the responding cortex occupied regions buried in the medial wall of the coronal sulcus. This interpretation is consistent with the demonstrations by previous receptive-field mapping studies that in some but not all cats, a portion of the SI central-pad representational area can lie within cortex buried in the medial bank of the coronal sulcus (McKenna et al. 1981).

In striking contrast to the prominent SI optical responses obtained in subjects with 25-Hz stimulation, stimulation of the same central-pad site with the 200-Hz stimulus failed to evoke a discernable change in absorbance in either area 3b or area 1 (compare Fig. 3, *middle* with *left*). Instead, in the three subjects whose data are shown in Fig. 3, 200-Hz stimulation was accompanied only by an extremely weak absorbance increase in area 3a (e.g., the response in area 3a to 200-Hz stimulation is most apparent in *subject 2* in Fig. 3).

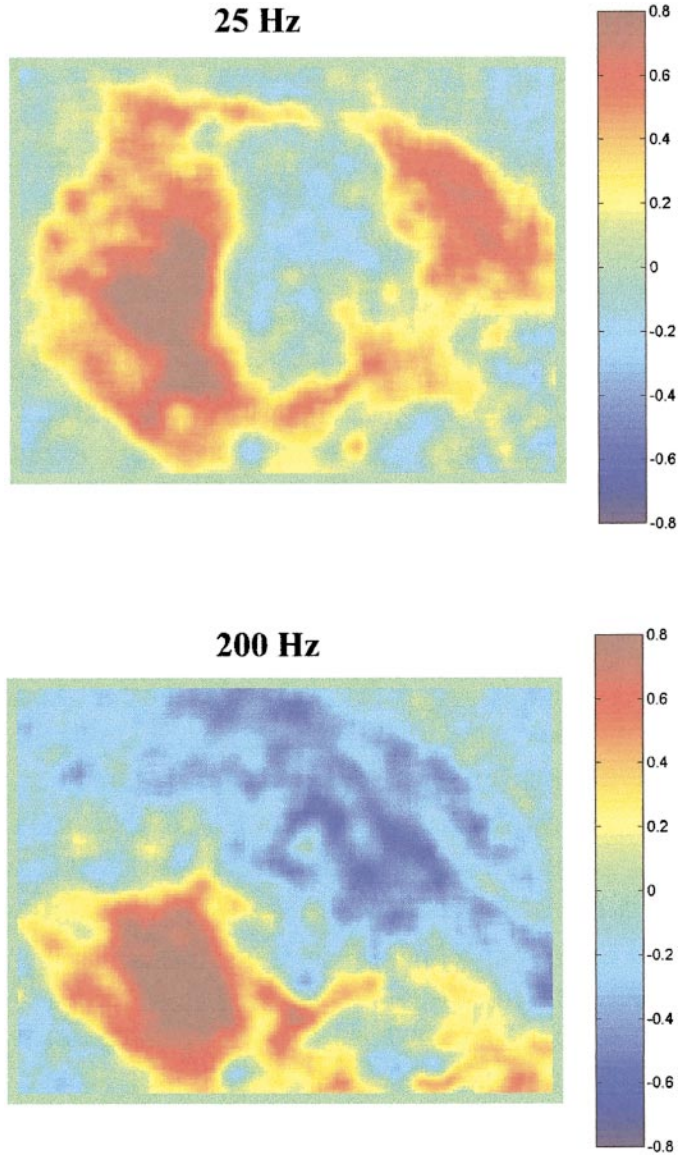


FIG. 7. Correlation maps generated from OIS-imaging data obtained from subject (*subject 1*) whose data are shown in Fig. 5. *Top*: obtained from the data acquired under 25-Hz stimulation; *bottom*: obtained from the data acquired under 200-Hz stimulation. Color scale (*right*) indicates the value of the correlation coefficient. Each map was obtained by computing the correlation (estimated by the correlation coefficient, *r*) between the changes in absorbance over time at each pixel location and the time course of the increase in average absorbance within the SII boxel that exhibited the maximal absorbance increase during the delivery of the appropriate stimulus frequency. For each map the value of [*r*] that had to be exceeded to be regarded as significantly different from 0 ($P < 0.05$): map at *top* (0.4 4); map at *bottom* (0.45). Note that under the 200-Hz stimulus condition, the activity in most locations in the SI forelimb region is anticorrelated with the time course of the absorbance change that the 200-Hz stimulus evokes in the maximally activated boxel within SII—see *bottom;* whereas under the 25-Hz condition, the activity at most sites in both SI and SII is positively correlated with the time course of the absorbance change that the 25-Hz stimulus evokes within the maximally activated SII boxel (*top*).

Figure 4 shows results obtained in two OIS-imaging experiments in which the central-pad representational area in *both* SI and SII in the contralateral hemisphere were imaged simultaneously in response to interleaved trials of 25- and 200-Hz stimulation. Fig. 4, *top*, shows, for both subjects, the responses of the contralateral SI and SII 5 s after onset of a 25-Hz

stimulus. The images in Fig. 4, *middle,* show the responses obtained from SI and SII of the same two subjects 5 s after onset of a 200-Hz stimulus to the same central-pad site. Comparison of the images in the *top two rows* in Fig. 4 makes it obvious that although SI in both subjects (SI is located at the *top right* of the field imaged in both experiments; SII is located at the *left* of each field) underwent a prominent increase in absorbance in response to the 25-Hz central-pad stimulus condition, SI did not. More specifically, *subject 1* exhibited little or no increase in SI absorbance in response to same-site 200-Hz stimulation (*middle left*), and although a small increase in SI absorbance did occur in *subject 2* (*middle right*), it does not approach the magnitude of the increase in absorbance evoked in SI of the same subject by same-site 25-Hz stimulation.

Although Fig. 4 makes it apparent that SII underwent a large increase in absorbance in response to both the 25- and 200-Hz stimuli, it is interesting that the region in SII that responded with an absorbance increase is not the same for the two stimulus frequencies. In both subjects whose data are seen in Fig. 4, the SII region that responded to 200-Hz stimulation only partially overlaps the region that responded to 25-Hz stimulation—the territory that responds to 200 Hz is located slightly more posterior than the one that responds to 25-Hz stimulation. This difference in the SII locus of the responses to 25- and 200-Hz stimulation is most apparent when (see Fig. 5, *top*) the difference images obtained from each subject under the two stimulus conditions are thresholded and superimposed (in the thresholded images, gray = the SI and SII areas responding to 200 Hz and black = SI and SII areas responding to 25 Hz).

Because the OIS images in Figs. 3 and 4 only show the responses of SI and SII at single time (5 s) after stimulus onset, the time course of the SI and SII responses to each stimulus frequency was evaluated to determine if, and to what extent, the responses modify with time after stimulus onset. The following three-step procedure was used. First, the 2 × 2 mm boxel within SI that exhibited the largest increase in average absorbance at 5 s after onset of 25-Hz stimulation and the 2 × 2mm boxel within SII that exhibited the maximal absorbance increase to the same stimulus condition were identified. Second, the average absorbance value within the same SI and SII boxels were determined for each difference image acquired after the onset of each stimulus frequency. And third, average absorbance in each boxel was plotted as a function of time after stimulus onset.

The graphs in Fig. 5 (*left*: *subject 1; right*: *subject 2*) show, for the same two subjects whose data are shown in Fig. 4, the time course of the absorbance change within the abovementioned SI and SII boxels during 25-Hz stimulation (plotted using heavy lines) and during 200-Hz stimulation of the central pad (plotted using thin lines). For *subject 1* the duration of both the 25- and 200-Hz stimuli was 10 s; it was 20 s for *subject 2.* The graphs in Fig. 5 clearly reveal that in each subject 25-Hz stimulation evoked an increase in absorbance in both the SI and SII boxels and that the increase in absorbance evoked by 25-Hz stimulation in both the SI and SII boxels developed relatively rapidly after stimulus onset. Moreover, they show that in the SI and SII boxels in both subjects absorbance is near-maximal within 3–5 s of onset of 25-Hz stimulation and declines to ~65–80% of its maximal value with continuing stimulation. Two hundred-Hz stimulation, like 25-Hz stimulation, evoked in both subjects a prominent and rapidly developing increase in absorbance in the SII boxel, but unlike 25-Hz stimulation, elicited only a weak and slow-to-develop increase in absorbance in the SI boxel in *subject 2* and a biphasic change in absorbance (a weak increase at 1 s after stimulus onset, followed by a frank decrease) in the SI boxel in *subject 1.*

Figure 6 shows that very similar findings obtained from the contralateral SI in three additional subjects studied with the OIS-imaging method (see legend to Fig. 6 for details). In general, the findings obtained from the five subjects whose data are shown in Figs. 5 and 6 indicate the considerable across-subject consistency of the prominent, but very different, optical responses of the contralateral SI to same-site 25- and 200-Hz stimulation.

The next and final approach we used to analyze the OIS-imaging data was correlation mapping. More specifically, the method of correlation mapping was used *1*) to obtain an outcome (a correlation map) for each stimulus condition that provides an objective measure (a correlation value) of the association between the time course of the change in absorbance within the region of maximal activity and the time course of change in absorbance at each pixel location outside the maximally activated region, *2*) to objectively specify the outcome of functional interactions between cortical regions in terms of the value and sign of the measured correlation, and *3*) to assess the statistical significance of the correlation measured at each cortical site (see Tommerdahl et al. 1998).

Maps showing the correlation between the time course of the change in absorbance at each pixel location with those that occurred within the maximally activated boxel in SII were generated for the two subjects in whom SI and SII in the same hemisphere were imaged simultaneously (see Figs. 4 and 5)—for each of these subjects, a correlation map was generated using the data obtained under the 25-Hz stimulus condition and also using the data obtained under the 200-Hz condition. Figure 7 shows the correlation maps generated from the data of *subject 1* obtained under 25-Hz stimulation (*top*) and under 200-Hz stimulation (*bottom*).

Inspection of the correlation map generated for the 25-Hz condition (Fig. 7, *top*) reveals that under this condition the activities in extensive areas (indicated in red) in both SI and SII in the contralateral hemisphere are *highly positively correlated* with the increase in absorbance that occurred in the maximally activated SII boxel. In contrast, the correlation map generated for the 200-Hz condition (Fig. 7, *bottom*) shows that under this condition the activity within an extensive region of SII and the fields that border it (e.g., area SIV) is correlated positively (shown in red) with the increase in absorbance that occurs in the maximally activated SII boxel, whereas the activity in much of SI is *highly and significantly anticorrelated* (indicated in blue) with the time course of the activity in the SII boxel. The correlation maps generated in the same way from the other subject (*subject 2;* see Fig. 4) exhibited characteristics similar to those of the maps in Fig. 7.

## DISCUSSION

### *Effects of high-frequency skin stimulation on the contralateral SI*

The 2DG- and the OIS-imaging observations from cat SI closely parallel the results obtained recently in a study of SI in squirrel monkeys (Tommerdahl et al. 1999). That study

showed that a 1- to 5-s 25-Hz skin stimulus evokes a prominent, well-maintained absorbance increase in the topographically appropriate locus in contralateral area 3b and/or area 1, whereas delivery of 200-Hz stimulation to the same skin site results in only a weak and transient increase in absorbance at the same SI locus. In addition, it was shown that as stimulus duration increased, the difference between the squirrel monkey SI optical responses evoked by 25- versus 200-Hz stimulation becomes progressively more distinct. In particular, with 25-Hz stimulation, a large absorbance increase developed rapidly and was relatively well maintained as long as the stimulus was continued. In contrast, with 200-Hz stimulation, an early, weak increase in absorbance occurred, but within 3–5 s of stimulus onset, it was replaced by a prominent and spatially extensive region of decreased absorbance that persisted until stimulation was discontinued (Tommerdahl et al. 1999).

Neither the OIS- nor the 2DG-imaging results reported in this study, nor the findings reported by Tommerdahl et al. (1999) in squirrel monkey SI, are easily accommodated with one component of the long-held view (Hyvarinen et al. 1968; Mountcastle et al. 1967, 1969, 1990; Talbot et al. 1968; for review, see Mountcastle 1984) that dual neural mechanisms in SI cortex underlie the capacities to detect and discriminate frequency of vibrotactile stimulation. Specifically, the data appear at conflict with the idea that a distinct class of SI neurons signals by either a periodicity or mean rate code, the higher stimulus frequencies ($>$60 Hz) at which humans experience vibration.

It should be noted that a number of findings in the published literature, similar to the observations reported in this paper, also are not easily accommodated with the idea that it is the PC-type SI neurons that encode the frequency of skin stimulation over the range which humans experience as vibration. First, Mountcastle et al. (1969) demonstrated in their elegant initial study of the cortical mechanisms in flutter-vibration that neither the overall mean firing rate nor any periodic ordering of the spikes discharged by PC-type SI neurons provides a discriminable signal of frequency at stimulus frequencies between 100 and 200 Hz. Second, Lebedev et al. (1994) reported that during the delivery of 127-Hz stimulation to the contralateral palm the mean firing rate (MFR) of SI neurons in conscious behaving monkeys is significantly lower than the firing rates evoked at 27 and 57 Hz—a finding that led Lebedev et al. (1994) to conclude that the "decrease in MFR of neurons with cutaneous RFs at 127 Hz may be due to inhibitory mechanisms dependent on stimulus frequency." Third, in cats, high-frequency ($\geq$200 Hz) skin stimuli have been reported to activate SII neurons far more effectively than SI neurons (McIntyre et al. 1967; Rowe et al. 1985). And fourth, Pertovaara and Hamalainen (1981) interpreted their human psychophysical evidence to indicate that long-duration high-frequency skin stimuli inhibit the detection of low-frequency stimuli.

Although it is true that the preceding observations, either individually or collectively, do not permit conclusions about the detailed nature of the neuronal processes triggered in SI cortex by high-frequency skin stimulation, all appear generally consistent with the possibilities that the effects of 200-Hz skin stimulation on SI *1*) are more complex than would be anticipated if the SI mechanisms subserving flutter-vibration consisted solely of dual, independent neuron populations, each devoted exclusively to processing the afferent drive arising in one class (either the RA- or PC-type) of skin mechanoreceptors and *2*) involve a potent, spatially widespread, and generalized inhibitory influence on SI neurons. The latter possibility is viewed as fully consistent with the observation that SI and SII activities are highly negatively correlated (see Fig. 7) under the condition of 200-Hz skin stimulation.

### *Interdependencies between SI and SII*

The available literature indicates that SII derives the major component of its input from SI in the same hemisphere in macaque monkeys (Pons et al. 1987) but receives its principal input from the thalamus in cats (Alloway et al. 1988; Bennett et al. 1980; Ferrington and Rowe 1980; Fisher et al. 1983; Herron and Dykes 1986). Although this prominent species difference in SII afferent connectivity has been proposed to indicate that in monkey SII occupies a higher position in the somatosensory information processing hierarchy than in cat (Pons et al. 1987), others have warned that "these are basically descriptive schemes of connections that do not illuminate what features of somesthesis are selectively projected" and that "they also tend to ignore potential interdependence between SI and SII" (Burton and Sinclair 1991).

The OIS observations obtained in the present study by simultaneously imaging the contralateral SI and SII in cats during 200-Hz stimulation of the central pad (Figs. 4, 5, and 7) revealed that the time course of the optical response (increasing absorbance) evoked in SII is strongly and significantly negatively correlated with the time course of the optical signal in the region of the topographically appropriate region of SI. A plausible (but not necessarily correct) explanation for this outcome is that the activity evoked in SII exerts an inhibitory influence on SI via the extensive corticocortical connections known (Burton et al. 1995) to link topographically corresponding regions in the two areas. At the same time, the observations obtained during 25-Hz stimulation suggest (see Figs. 4, 5, and 7) that SI and SII in cat may function relatively more independently under this stimulus condition.

It is important to emphasize that the data presented in this paper cannot be used to evaluate any particular model of information flow (e.g., the serial vs. parallel models of information flow). These models address the sources of the information that reaches SI and SII, whereas the data presented in this paper address a completely different issue—whether, and to what extent, the responses of SI and SII in the same hemispheres are independent.

The data presented show that nonnoxious mechanical skin stimulation (both low and high frequency) evoke afferent activity that is conveyed via central somatosensory paths to *both* SI and SII in the contralateral hemisphere and raise the possibility that unlike the activity evoked by cutaneous flutter, the vigorous SII activity generated by high-frequency skin stimulation (vibration) may depress (perhaps via inhibitory processes mediated by cortico-cortical connections) the response of SI to ongoing skin stimulation. Thus one possible interpretation is that SII activity levels mediate SI response, particularly when these activity levels have been evoked by vibratory stimuli. The findings appear to require the conclusion that, at least in cat the degree to which SI and SII in the contralateral hemisphere contribute to the somatosensory cortical response to skin stimulation is frequency-dependent with SII making a

progressively greater and SI a progressively lesser contribution to the response of the contralateral hemisphere as stimulus frequency is increased >25 Hz.

The authors acknowledge the expert technical support of C. Wong.

M. Tommerdahl was supported in part by National Institute of Neurological Disorders and Stroke (NINDS) R29 Grant NS-32358. The experiments were funded by NINDS RO1 Grant NS-34979 (B. L. Whitsel).

Address for reprint requests: M. Tommerdahl, Dept. of Biomedical Engineering, University of North Carolina, CB# 7575, Chapel Hill, NC 27599.

Received 16 February 1999; accepted in final form 27 May 1999.

## REFERENCES

ALLOWAY, K. D., SINCLAIR, R. J., AND BURTON, H. Responses of neurons in somatosensory cortical area II of cats to high frequency vibratory stimuli during iontophoresis of a GABA antagonist and glutamate. *Somatosens. Res.* 6: 109–140, 1988.

BENNETT, R. E., FERRINGTON, D. G., AND ROWE, M. Tactile neuron classes with second somatosensory area (SII) of cat cerebral cortex. *J. Neurophysiol.* 43: 292–309, 1980.

BERGLUND U. AND BERGLUND. Adaptation and recovery in vibrotactile perception. *Percept. Mot. Skills* 30: 843–853, 1970.

BURTON, H., FABRI, M., AND ALLOWAY, K. Cortical areas within the lateral sulcus connected to cutaneous representations in areas 3b and 1: a revised interpretation of the second somatosensory area in macaque monkeys. *J. Comp. Neurol.* 355: 539–562, 1995.

BURTON, H., MITCHELL, G., AND BRENT, D. Second somatic sensory area in the cerebral cortex of cats: somatotopic organization and cytoarchitecture. *J Comp. Neurol.* 210: 109–135, 1982.

BURTON, H. AND SINCLAIR, R. J. Second somatosensory cortical area in macaque monkeys. II. Neuronal responses to punctate vibrotactile stimulation of glabrous skin on the hand. *Brain Res.* 538: 127–135, 1991.

EBNER, T. J. AND CHEN, G. Use of voltage sensitive dyes and optical recordings in the central nervous system. *Prog. Neurobiol.* 46: 463–506, 1995.

FERRINGTON, D. G. AND ROWE, M. J. Differential contributions to the coding of cutaneous vibratory information by cortical somatosensory areas I and II. *J. Neurophysiol.* 43: 310–331, 1980.

FISHER, G. R., FREEMAN, B., AND ROWE, M. J. Organization of parallel projections from pacinian afferent fibers to somatosensory cortical areas I and II in the cat. *J. Neurophysiol.* 49: 75–97, 1983.

GARRAGHTY, P. E., PONS, T. P., AND KAAS, J. H. Ablations of areas 3b (S-I proper) and 3a of somatosensory cortex in marmosets deactivate the second and parietal ventral somatosensory areas. *Somatosens. Mot. Res.* 7: 125–135, 1990.

GRINVALD, A. Real-time optical mapping of neuronal activity: from single growth cones to the intact mammalian brain. *Annu. Rev. Neurosci.* 8: 263–305, 1985.

GRINVALD, A., BONHOEFFER, T., MALONEK, D., SHOHAM, D., BARTFELD, E., ARIELI, A., HILDESHEIM, R., AND RATZLAFF, E. Optical imaging of architecture and function in the living brain. In: *Memory Organization and Locus of Change*, edited by L. Squire, N. Weinberger, G. Lynch, and J. McGaugh. New York: Oxford Univ. Press, 1991, p. 49–85.

GRINVALD, A. LIEKE, E. E., FROSTIG, R. D., AND HILDESHEIM, R. Cortical spread-point function and long-range lateral interactions revealed by real-time optical imaging of macaque monkey primary visual cortex. *J. Neurosci.* 14: 2545–2568, 1994.

HASSLER, R. AND MUHS-CLEMENT, K. Architektonischer Aufbau des sensomotorischen und parietalen Cortex der Katze. *J. Hirnforsch.* 6: 377–420, 1964.

HERRON, P. AND DYKES, R. W. Connections and function of the thalamic ventroposterior inferior (VPI) nucleus in cats: a relay nucleus in the Pacinian pathway to somatosensory cortex. *J. Neurophysiol.* 56: 1475–1497, 1986.

HYVARINEN, J., SAKATA, H, TALBOT, W. H., AND MOUNTCASTLE, V. B. Neuronal coding by cortical cells of the frequency of oscillating peripheral stimuli. *Science* 162: 1130, 1968.

JULIANO, S. L., HAND, P. J., AND WHITSEL, B. L. Patterns of increased metabolic activity in somatosensory cortex of monkeys, *Macaca fascicularis*, subjected to controlled cutaneous stimulation. *J. Neurophysiol.* 46: 1260–1284, 1981.

JULIANO, S. L., HAND, P. J., AND WHITSEL, B. L. Patterns of metabolic activity in cytoarchitectural area SII and surrounding cortical fields of the monkey. *J. Neurophysiol.* 50: 961–980, 1983.

LEBEDEV, M. A., DENTON, J. M., AND NELSON, R. J. Vibration-entrained and premovement activity in monkey primary somatosensory cortex. *J. Neurophysiol.* 72: 1654–1673, 1994.

LEBEDEV, M. A. AND NESON, R. J. High-frequency vibratory sensitive neurons in monkey primary somatosensory cortex: entrained and non-entrained responses to vibration during the performance of vibratory-cued hand movements. *Exp. Brain Res.* 111: 313–325, 1996.

MCINTYRE, A. K., HOLMAN, M. E., AND VEALE, J. L. Cortical responses to impulses from single Pacinian corpuscles in the cat's hindlimb. *Exp. Brain Res.* 4: 243–244, 1967.

MCKENNA, T. M., WHITSEL, B. L., DREYER, D. A., AND METZ, C. B. Organization of cat anterior parietal cortex: relations among cytoarchitecture, single neuron functional properties and interhemispheric connectivity. *J. Neurophysiol.* 45: 667–697, 1981.

MOUNTCASTLE, V. B. Central nervous mechanisms in mechanoreceptive sensibility. In: *Handbook of Physiology. The Nervous System. Sensory Processes.* Bethesda, MD: Am. Physiol. Assoc., 1984, sect. 1, vol. III, p. 789–878.

MOUNTCASTLE, V. B., LAMOTTE, R. H., AND CARLI, G. Detection thresholds for stimuli in humans and monkeys: comparison with threshold events in mechanoreceptive afferent nerve fibers innervating the monkey hand. *J. Neurophysiol.* 35: 122–136, 1972.

MOUNTCASTLE, V. B., STEINMETZ, M. A., AND ROMO, R. Frequency discrimination in the sense of flutter psychophysical measurements correlated with postcentral events in behaving monkeys. *J. Neurosci.* 10: 3032–3044, 1990.

MOUNTCASTLE, V. B., TALBOT, W. H., DARIAN-SMITH, I., AND KORNHUBER, H. H. A neural basis for the sense of flutter-vibration. *Science* 155: 597–600, 1967.

MOUNTCASTLE, V. B., TALBOT, W. H., SAKATA, H., AND HYVARINEN, H. Cortical neuronal mechanisms in flutter vibration studied in unanesthetized monkeys: neuronal periodicity and frequency discrimination. *Neurophysiology* 32: 452–484, 1969.

PERTOVAARA, A. AND HAMALAINEN, H. Vibrotactile thresholds during vibration of long duration. *Scand. J. Psychol.* 22: 41–45, 1981.

PONS, T. P., GARRAGHTY, P. E., FRIEDMAN, D. P., AND MISHKIN, M. Physiological evidence for serial processing in somatosensory cortex. *Science* 237: 417–420, 1987.

ROWE, M. J. Impulse patterning in central neurons for vibrotactile coding. In: *Information Processing In Mammalian Auditory and Tactile Systems*. New York: A. R. Liss, 1990, p. 111–125.

ROWE, M. J., FERRINGTON, D. G., FISHER, G. R., AND FREEMAN, B. Parallel processing and distributed coding for tactile vibratory information within sensory cortex. In: *Development, Organization, and Processing In Somatosensory Pathways*. New York: A. R. Liss, 1985, chapt. 27, p. 247–258.

ROWE, M. J., TURMAN, A. B., MURRAY, G. M., AND ZHANG, H. Q. Parallel processing in somatosensory areas I and II of the cerebral cortex. In: *Somethesis and the Neurobiology of the Somatosensory Cortex*, edited by O. Franzen, R. Johannsson, and L. Terenius. Basel: Birkhauser Verlag, 1996, p. 197–212.

TOMMERDAHL, M. *Stimulus-Evoked Activity Patterns in the SI Cortex* (PhD thesis). Chapel Hill, NC: University of North Carolina , 1989.

TOMMERDAHL, M., BAKER, R., WHITSEL, B. L., AND JULIANO, S. L. A method for reconstructing patterns of somatosensory crebral cortical activity. *Biomed. Sci. Instrum.* 21: 93–98, 1985.

TOMMERDAHL, M., DELEMOS, K. A., FAVOROV, O. V., METZ, C. B, VIERCK, C. J., JR., AND WHITSEL, B. L. Response of anterior parietal cortex to different modes of same-site skin stimulation. *J. Neurophysiol.* 80: 3272–3283, 1998.

TOMMERDAHL, M., DELEMOS, K. A., WHITSEL, B. L., FAVOROV, O. V. AND METZ, C. B. The response of anterior parietal cortex to cutaneous flutter and vibration. *J. Neurophysiol.* 82: 16–33, 1999.

TOMMERDAHL, M., FAVOROV, O. V., WHITSEL, B. L., NAKHLE, B., AND GONCHAR, Y. A. Minicolumnar activation patterns in cat and monkey SI cortex. *Cereb. Cortex* 3: 399–411, 1993.

TOMMERDAHL, M. AND WHITSEL, B. L. Optical imaging of intrinsic signals in somatosensory cortex. In: *Somesthesis and the Neurobiology of Somatosensory Cortex*, edited by O. Franzen, R. Johansson, and L. Terenius. Basel: Birkhauser Verlag, 1996, p. 369–384.

TOMMERDAHL, M., WHITSEL, B. L., VIERCK, C. J., JR., FAVOROV, O., JULIANO, S., COOPER, B., METZ, C., AND NAKHLE, B. Effects of spinal dorsal column transection on the response of monkey anterior parietal cortex to repetitive skin stimulation. *Cereb. Cortex* 6: 131–155, 1996.